

# Ferroelectric–relaxor crossover characteristics in $\text{Ba}(\text{Zr}_x\text{Ti}_{1-x})\text{O}_3$ ceramics investigated by AFM-piezoresponse study

Dan Ricinski<sup>a</sup>, Cristina Elena Ciomaga<sup>b</sup>, Liliana Mitoseriu<sup>b,\*</sup>,  
Vincenzo Buscaglia<sup>c</sup>, Masanori Okuyama<sup>a</sup>

<sup>a</sup> Osaka University, Graduate School of Eng. Science, Dept. of Systems Innovation, 1-3, Machikaneyama-cho, Toyonaka, Osaka 560-8531, Japan

<sup>b</sup> Dept. of Solid State & Theor. Physics, Al. I. Cuza Univ., Bv. Carol I no. 11, Iasi 700506, Romania

<sup>c</sup> Institute for Energetics & Interphases IENI - CNR, Via de Marini no. 6, Genoa I-16149, Italy

Available online 25 June 2009

## Abstract

$\text{Ba}(\text{Zr}_x\text{Ti}_{1-x})\text{O}_3$  ceramics with  $x=0.10$  and  $0.18$  prepared via solid state, with high-density, homogeneous microstructures and similar grain size were investigated. The dielectric data showed that the relaxor properties are induced by increasing the Zr vs. Ti fraction  $x$ , both compositions showing a combined relaxor–ferroelectric character. The AFM-piezoresponse experiments revealed a few interesting characteristics, as follows: (1) none of the samples could be totally poled or switched, like the normal ferroelectrics; (2) the samples locally present different types of responses (ferroelectric with a strong piezoresponse, field-induced ferroelectric, polar but non-switchable and non-polar regions); (3) both the regions with a natural strong piezoresponse and the ones obtained after poling are larger in size and more stable in time for the sample with  $x=0.10$  than for  $x=0.18$ ; (4) the sample having  $x=0.18$  has a smaller piezoresponse than the one with  $x=0.10$ . The observed local features are confirming the ferroelectric–relaxor crossover with increasing  $x$ , as observed by the analysis of the dielectric data.

© 2009 Elsevier Ltd. All rights reserved.

**Keywords:** Dielectric properties; Ferroelectric properties;  $\text{BaTiO}_3$ ; Titanates

## 1. Introduction

A large number of  $\text{BaTiO}_3$ -based solid solutions have been studied in the last years due to environmental concerns which are driving the exploration for new Pb-free piezo/ferroelectric materials with superior performances.<sup>1,2</sup> Substitution of other ions for host cations at the A or B site in  $\text{BaTiO}_3$  perovskite cell leads to remarkable changes of its characteristics.<sup>3,4</sup> Despite the fact that it was discovered in the sixties and being a main constituent of the commercialized multilayer ceramic capacitors (Z5U, Y5V<sup>2</sup>), the system  $\text{Ba}(\text{Zr}_x\text{Ti}_{1-x})\text{O}_3$  (BZT) became interesting for more fundamental studies and also for some novel applications, due to the excellent dielectric, tunability and promising piezoelectric/electrostrictive properties.<sup>5–11</sup> The ferroelectric properties of BZT are largely dependent on the amount of Zr substitution.<sup>6,7,11</sup> The system exhibits a pinched phase transition with increasing Zr concentration (at  $x \approx 0.15$ , the three phase transitions are merged into one broad peak). Normal fer-

roelectric behavior for  $0 < x < 0.10$ , relaxor when  $x > 0.25$  and antiferroelectric properties for high Zr addition were observed. These limits are sensitive to the preparation method, the presence of secondary phases and to microstructural characteristics as porosity degree, grain size, etc.<sup>6,7,12,13</sup> To characterize the ferroelectric–relaxor crossover, the dielectric data obtained at various frequencies are typically used. In the present paper, in addition to the dielectric study of  $\text{Ba}(\text{Zr}_x\text{Ti}_{1-x})\text{O}_3$  ceramics, a careful AFM-piezoresponse investigation was undertaken in order to find peculiar local switching characteristics induced by increasing  $x$ . Ceramics with  $x=0.10$  and  $0.18$  prepared via solid state, with high-density, homogeneous microstructures and similar grain size were selected to be comparatively investigated by this method.

## 2. Experiment

Pure perovskite  $\text{Ba}(\text{Zr}_x\text{Ti}_{1-x})\text{O}_3$  ceramics were prepared by solid-state reaction technique, as described in Refs. [12,13]. The microstructures were characterized by scanning electron microscopy (SEM, LEO 1450VP, LEO Electron Microscopy

\* Corresponding author. Tel.: +40 232201175; fax: +40 232201205.  
E-mail address: [lmstr@uaic.ro](mailto:lmstr@uaic.ro) (L. Mitoseriu).

Ltd., Cambridge, UK). The electrical characterization was performed in plan-parallel configuration on the polished (down to 0.5 mm) and electroded (Ag–Pb) samples by using a Solartron SI1260 impedance analyzer in the frequency range 1–10<sup>6</sup> Hz at temperatures of 30–200 °C with a heating/cooling rate of 0.5 °C/min. Nanoscale switching characterization was performed by using a FCE ferroelectric tester (Toyotecnica) which can alternatively be connected to a conventional needle probe as well to an Autoprobe CP-R multitask AFM (PSI, Veeco) via a lock-in amplifier or an amplifier with fast offset cancel.<sup>14</sup> As AFM tips, Si cantilevers coated with Rh, with a large elastic constant of 20 N/m have been used. In order to confirm the polarization reversal mechanism at local scale, a sequence of poling-imaging experiments on a 25 μm<sup>2</sup> area of the ceramic (its size was selected so that it includes several grains), was performed. The entire area has been initially pre-poled with upward-oriented polarization by scanning with a bias voltage of –200 V applied to the AFM tip. The polarization reversal was afterwards induced in the previously poled area by applying a +200 V bias voltage. The typical piezoresponse force microscopy technique (PFM) has been used for the domain imaging experiments in each state. We have used the in-phase Acos(φ) signal measured by the lock-in amplifier for a 1.1 kHz reference signal.

### 3. Results and discussions

The SEM micrographs of the investigated BZT ceramics presented in Fig. 1a and b show dense and homogeneous microstructures, with average grain sizes of ~3.3 μm for  $x = 0.10$  and ~1.54 μm for  $x = 0.18$  compositions.

The dielectric permittivity of the Ba(Zr<sub>x</sub>Ti<sub>1-x</sub>)O<sub>3</sub> ceramics with  $x = 0.10$  and 0.18 for a few frequencies is shown in Fig. 2a and b. The composition  $x = 0.10$  (Fig. 2a) shows a permittivity vs. temperature dependence with a well-defined maximum located at around  $T_m \approx 90$  °C, with almost no shift when the frequency increases and slightly diffuse character. In the ferroelectric phase (for  $T < T_m$ ), the permittivity presents a relaxation in the range of (1–0.5 × 10<sup>5</sup>) Hz. As expected,<sup>5–7,11</sup> the relaxor character is predominant for higher Zr addition. The composition  $x = 0.18$  has a more diffuse phase transition with a higher shift of the temperature corresponding to the permittivity maximum  $T_m \approx 60$  °C (Fig. 2b) with increasing frequency. Therefore, both samples show a mixed relaxor–ferroelectric character, with a higher weight of the relaxor state when increasing  $x$ . This is also demonstrated by the results of fits with the empirical equation<sup>15</sup>:

$$\varepsilon = \frac{\varepsilon_m}{1 + ((T - T_m)/\delta)^\eta}, \quad (1)$$

where the parameter  $\delta$  is related to the temperature extension of the phase transition and  $\eta \in (1, 2)$  is a parameter giving information on the character of the phase transition ( $\eta = 1$  for full ferroelectric state with Curie–Weiss law, while  $\eta = 2$  describes a complete diffuse phase transition and full relaxor behavior). The fits of the dielectric data at the frequency  $f = 80$  kHz gave the values:  $\eta = 1.5$  and  $\delta = 20$  °C for  $x = 0.10$  and  $\eta = 1.7$  and  $\delta = 36$  °C for  $x = 0.18$  demonstrated that both compositions

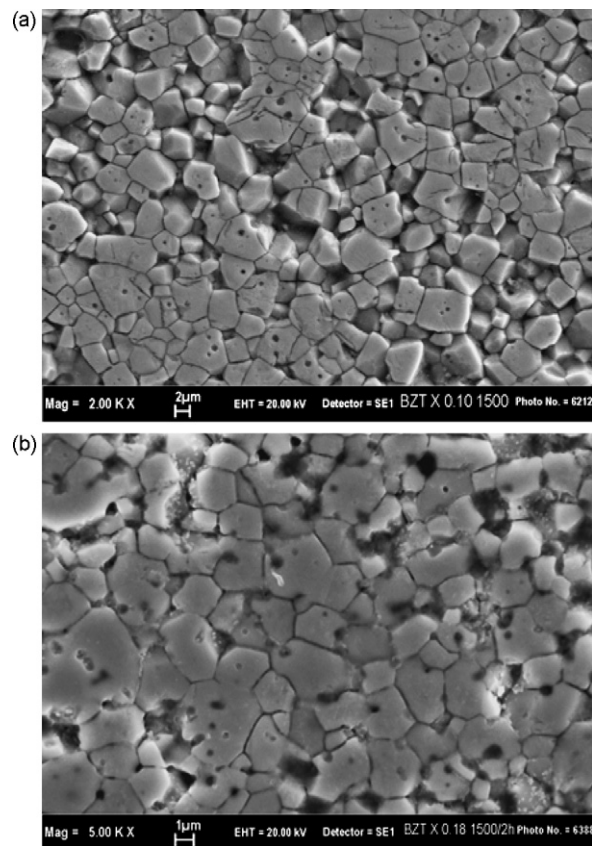


Fig. 1. Surface SEM images of: (a) BaZr<sub>0.10</sub>Ti<sub>0.90</sub>O<sub>3</sub> (bar = 2 μm) and (b) BaZr<sub>0.18</sub>Ti<sub>0.82</sub>O<sub>3</sub> (bar = 1 μm) ceramics sintered at 1500 °C/2 h.

have a mixed ferroelectric–relaxor character and the increasing relaxor character with increasing the Zr content. However, further analysis based on the Vogel–Fulcher laws usually used to describe the ferroelectric–relaxor crossover is inadequate for the present data. Extrinsic effects (Maxwell–Wagner<sup>16</sup>) probably related to local stoichiometry variations (mainly related to oxygen vacancies) resulting in uncompensated bounded charges in the sample's volume give some contributions mainly at high temperatures. The present BZT solid solutions do indeed exhibit such a behavior, which manifests by a frequency-dependence of the dielectric constant in the paraelectric state (Fig. 2b). Due to such contributions, discussions on the relaxor character on the basis of the dielectric data only are improper.

At microscopic level, the relaxor character is related to the degree of order/disorder and the scale or coherence length of the ordered nanodomains.<sup>17</sup> The relaxors show a negligible macroscopic polarization, in spite of local polarized nanoregions with short range ordering (SRO). These nanoregions tend to grow and enlarge by decreasing the temperature, in a dynamical process. However, as they are inhibited by the quenched compositional fluctuations and by the induced random fields, they are unable to establish adequate interaction among the neighbors to result in a long range ordering (LRO) like true ferroelectrics. The system can be turned from a SRO relaxor into a LRO ferroelectric by applying an external field or by forming a solid solution with a ferroelectric. In the case of our system, from the ferroelectric state of BaTiO<sub>3</sub> ceramics, the addition of Zr breaks the LRO

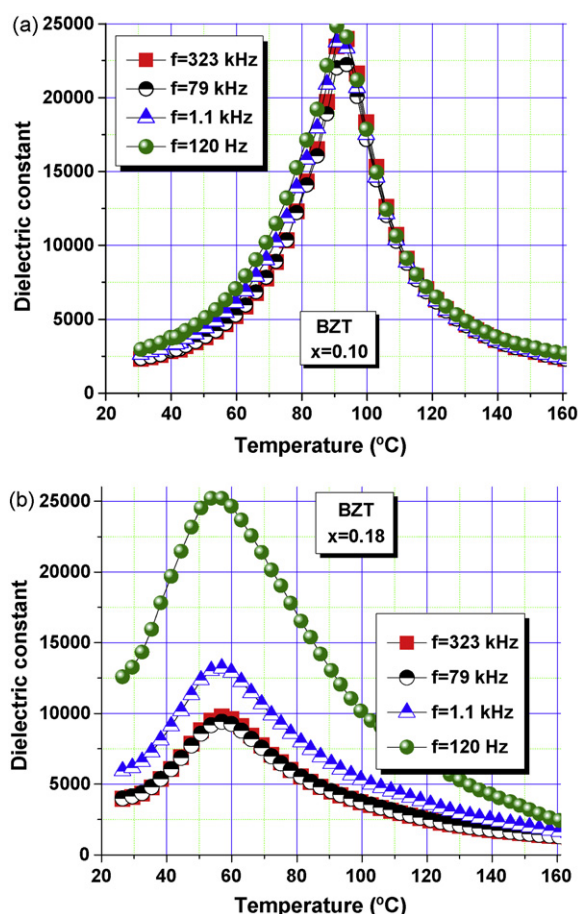


Fig. 2. Permittivity vs. temperature at a few frequencies in  $\text{Ba}(\text{Zr}_x\text{Ti}_{1-x})\text{O}_3$  ceramics with two compositions: (a)  $x=0.10$  and (b)  $x=0.18$ .

resulting in a SRO relaxor state. This trend should result in some characteristics of the switching properties at nanoscale that can be probed by PFM experiments. Similar domain imaging of ferroelectric relaxor ceramics by PFM technique has been performed by Kholkin et al.<sup>18</sup>

The domain structure of a  $25\ \mu\text{m}^2$  sample area, for a BZT ceramic with  $x=0.10$ , as resulted after a room temperature poling experiment consisting in scanning with negative and positive voltage applied to the conductive AFM tip, is presented in Fig. 4a and b. Simultaneous with the piezoelectric domain images, topography profiles of the two BZT ceramic samples have been acquired and are presented in Fig. 3. The poling was

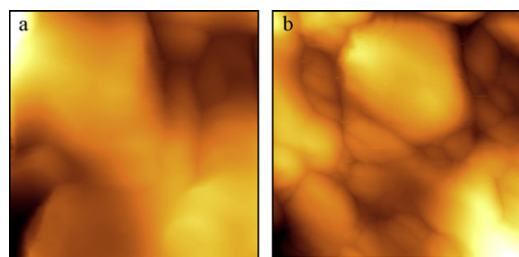


Fig. 3. AFM topography images for  $\text{Ba}(\text{Zr}_x\text{Ti}_{1-x})\text{O}_3$  ceramics with two compositions: (a)  $x=0.10$  and (b)  $x=0.18$ , taken simultaneously during PFM domain imaging experiments. Scan size is  $5\ \mu\text{m}$ .

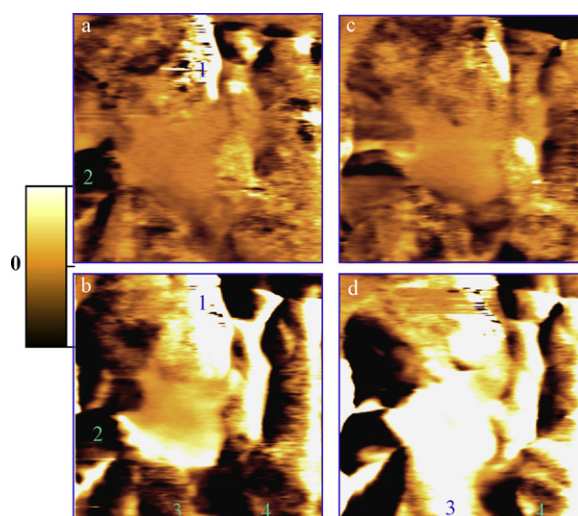


Fig. 4. Poling experiments of a surface area of  $25\ \mu\text{m}^2$  of  $\text{BaZr}_{0.10}\text{Ti}_{0.90}\text{O}_3$ : (a and c) negative voltage poling, (b and d) positive voltage poling by scanning with (a and b) 2 Hz and (c and d) 0.5 Hz frequency.

performed for about 2 min by the tip scanning (with a frequency of 2 Hz, yielding a poling time of about 1.95 ms/pixel) and the imaging around 15 min by scanning at 0.3 Hz. The domain structure obtained by the scanning fields with opposite orientations is well reproduced after repeating the experiment in similar conditions, showing that this is indeed a written domain structure and not artifacts due to any space charge effects. The high intensity poling field causes changes of the domains in the BZT ceramic sample (*i.e.* the contrast in Fig. 4a is mostly darkish while bright contrast domains are visible in central part of Fig. 4b). Overall, we remark that it was not possible to fully reverse the polarization by high field poling. Specifically, there are regions for which the domain contrast cannot be changed by the application of the scanning voltage. The marked regions maintain their bright (marked # 1) and respectively dark (marked # 2) contrast after the application of either way oriented bias scanning field. Such a behavior can be ascribed to frozen-in polarization region associated to some of the smaller grains visible in Fig. 3a, where possibly polar defects might pin the domain walls and impose a frozen-in polarization direction. A peculiar feature of these BZT ceramic sample is the presence of  $180^\circ$  domains in the state poled with positive voltage on the AFM tip. These are probably formed due to the residual depolarization field caused by incomplete penetration of domains over sample thickness. However, in the negatively poled state the domain contrast becomes intermediate, as in this case the polarization screening appears to be mediated by charged defects (oxygen vacancies) present in the sample volume that favor tail-to-tail vertical distribution of domains. In addition to the above-described structural distributions and domain interactions that are characteristic for a large class of normal ferroelectric materials, one cannot exclude the contribution of the Zr doping present in our ceramic samples to the observed domain patterns behavior: the SRO and the fluctuating polar nanoregions are also likely to prevent homogeneous contrast in PFM images.



A few further poling experiments were performed in same locations of the BZT sample with 10% Zr substitution in perovskite B-site positions. We have seen in Fig. 4b that the result of positive poling is to induce a bright contrast (corresponding to downward oriented remanent polarization) in the central part of the scanned area. Experiments performed in the same area with four times slower scanning frequencies during poling (0.5 Hz by comparison with 2 Hz, corresponding to 7.8 ms/pixel) demonstrated that a larger fraction of the scanned area can be switched by the same poling field if the poling time is longer (see Fig. 4c and d). The bright area is not confined to a single grain (although the reversed domains appears to nucleate close to the large grain boundary in Fig. 4b) as it enters several adjacent grains in Fig. 4d. These results demonstrate that the polarization regions within the BZT samples have rather distributed relaxation times (referring to the polarization relaxation and not to other charge relaxation processes possible present within the sample). Besides such regions, there are also zones that completely switch immediately, *i.e.* with small relaxation time, as there are regions keeping their original polarization irrespective of the larger poling time. These latter regions might have even higher relaxation times than the waiting time of these experiments. This complex behavior is probably related to the mixed relaxor–ferroelectric character of this composition, as demonstrated also by the dielectric results.

We have additionally measured dynamical piezoelectric displacement hysteresis loops (reversed butterflies strain–field curves) by connecting the conductive AFM tip to the ferroelectric tester via an amplifier with fast offset cancel. These experiments (data not shown here) consisted in point-by-point linear scanning over the sample surface every 100 nm, by a procedure similar with that described in Ref. [14]. Examining the field dependences of the piezoelectric displacement loops, we have identified three types of locations in our BZT ceramic sample: (i) typical ferroelectric regions with normal hysteresis loops, retaining their ferroelectricity after applying electric fields, with well-defined characteristics by repeating the experiment (saturation and coercive voltage); (ii) some regions initially not showing ferroelectric behavior turned into ferroelectric after the region was subjected to a few switching cycles. These are regions with a field-induced ferroelectric switching from an initial relaxor state; (iii) some regions that are never ferroelectric, neither before, nor after applying a large number of switching cycles. Although simultaneous PFM imaging was not performed in this experiment, the regions identified as (i) would be expected to appear with bright contrast as in the central part of Fig. 4b and d, those identified as (ii) to the regions marked with 3 in Fig. 4c and d, and those identified as (iii) to the regions marked with 1, 2 and 4 in Fig. 4b and d. These observations demonstrate a complex nanoscale switching behavior, with local inhomogeneity and mixed ferroelectric–relaxor character.

Similar experiments were performed for the  $x=0.18$  BZT composition, as seen from Fig. 5, with some particularities and differences mentioned below. For both compositions the domain structure does not usually correspond to the grain structure and morphology, *i.e.* one can find large grains with a multidomain structure or a group of small grains with the same domain

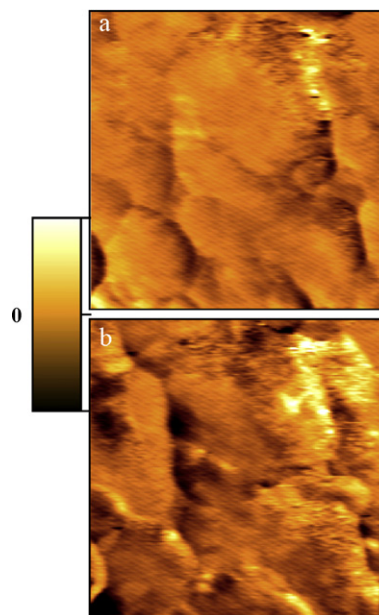


Fig. 5. Poling experiments of a surface area of  $25 \mu\text{m}^2$  of  $\text{BaZr}_{0.18}\text{Ti}_{0.82}\text{O}_3$ : (a) negative voltage poling and (b) positive voltage poling by scanning with 0.5 Hz frequency.

contrast. In particular, it is clearly demonstrated by comparing Figs. 4 and 5 that in a grain with a similar size, the spatial extent of ferroelectrically active areas is much smaller in a BZT ceramic sample with a high Zr content. This supports the assertion that the different behavior of the two types of ceramic samples is due to unit cell level breaking of long range order, as expected for relaxor materials, and not to any grain size effects.

A few important differences between the  $\text{BaZr}_{0.10}\text{Ti}_{0.90}\text{O}_3$  and  $\text{BaZr}_{0.18}\text{Ti}_{0.82}\text{O}_3$  ceramics were observed: (a) the composition  $x=0.18$  has a smaller piezoresponse than the ceramics with composition  $x=0.10$ , meaning an overall “lower ferroelectricity” for higher Zr addition; (b) the regions with a strong piezoresponse (attributed to natural ferroelectric regions) and the ones obtained after poling (attributed to regions with ferroelectricity induced by the poling field) are larger in size for the sample with  $x=0.10$  than for  $x=0.18$ ; (c) both the regions with natural and induced strong piezoresponse are more stable in time for the sample with  $x=0.10$  than for one with  $x=0.18$  (retention data not shown here). The fact that none of the two compositions cannot be totally switched even by high poling fields and after a long waiting time proves the “imperfect” ferroelectricity even in the sample  $x=0.10$ , considered by some authors in literature as being fully ferroelectric.<sup>6,11</sup> The lower piezoresponse, together with the smaller dimensions and lower stability of the ferroelectric domains for the sample  $x=0.18$  confirm the results of the dielectric data, *i.e.* the higher local polar disorder and higher relaxor character induced by higher Zr compositions. Extended studies regarding the relaxor characteristics and ferroelectric–relaxor phase transition in a more complete series of BZT ceramic samples are presented in Ref. [19].

#### 4. Conclusions

In the present work,  $\text{Ba}(\text{Zr}_x\text{Ti}_{1-x})\text{O}_3$  ceramics with  $x=0.10$  and  $0.18$  prepared via solid state, were comparatively investigated with the aim to evidence the role of Zr addition in inducing a predominant relaxor behavior. The dielectric data proved that both compositions show a combined relaxor–ferroelectric character and the relaxor properties are indeed enhanced by increasing the ratio of Ti substitution by Zr. The AFM-piezoresponse experiments revealed a few common characteristics, as follows: (1) none of the two compositions could be totally poled or switched, like the normal ferroelectrics and (2) the samples locally present different types of responses (ferroelectric with a strong piezoresponse, field-induced ferroelectric, polar but non-switchable and non-polar regions) and important differences: (i) the sample  $x=0.18$  has a smaller piezoresponse than  $x=0.10$  and (ii) the regions with a natural strong piezoresponse and ones obtained after poling are larger in size and more stable in time for the sample with  $x=0.10$  than for  $x=0.18$ . The local switching investigations confirm the conclusions of the dielectric study.

#### Acknowledgements

This work was supported by the Romanian CEEEX-FEROCER (2006–2008) and by Special Coordination Funds for Promoting Science and Technology of MEXT, Japan (YURAGI project of Osaka University).

#### References

- Saito, Y., Takao, H., Tani, T., Nonoyama, T., Takatori, K., Homma, T. et al., Lead-free piezoceramics. *Nature*, 2004, **432**, 84–87.
- Wolny, W. W., European approach to development of new environmentally sustainable electroceramics. *Ceram. Int.*, 2004, **30**, 1079–1083.
- Lines, M. E. and Glass, A. M., *Principles and Applications of Ferroelectrics and Related Materials*. Clarendon Press, Oxford, 1977.
- Böttger, U., Dielectric properties of polar oxides. In *Polar Oxides: Properties, Characterization and Imaging*, ed. R. Waser, U. Böttger and S. Tiedke. Wiley-VCH Verlag GmbH&Co. KGaA, Weinheim, 2005.
- Halder, S., Gerber, P., Schneller, T. and Waser, R., Electromechanical properties of  $\text{Ba}(\text{Ti}_{1-x}\text{Zr}_x)\text{O}_3$  thin films. *Appl. Phys. A*, 2005, **81**, 11–13.
- Simon, A., Ravez, J. and Maglione, M., Relaxor properties of  $\text{Ba}_{0.9}\text{Bi}_{0.067}(\text{Ti}_{1-x}\text{Zr}_x)\text{O}_3$  ceramics. *Solid State Sci.*, 2005, **7**, 925–930.
- Zhi, Y., Guo, R. and Bhalla, A. S., Dielectric behavior of  $\text{Ba}(\text{Ti}_{1-x}\text{Zr}_x)\text{O}_3$  single crystals. *J. Appl. Phys.*, 2000, **88**, 410–415.
- James, A. R. and Prakash, C., Ferroelectric properties of pulsed laser deposited  $\text{BaZr}_{0.15}\text{Ti}_{0.85}\text{O}_3$  thin films. *Appl. Phys. Lett.*, 2004, **84**, 1165–1167.
- Xu, J., Menesklou, W. and Ivers-Tiffée, E., Annealing effects on structural and dielectric properties of tunable BZT thin films. *J. Electroceram.*, 2004, **13**, 229–233.
- Zhi, Y., Ang, C., Guo, R. and Bhalla, A. S., Dielectric properties and high tunability of  $\text{BaTi}_{0.7}\text{Zr}_{0.3}\text{O}_3$  ceramics under dc electric field. *Appl. Phys. Lett.*, 2002, **81**, 1285–1287.
- Hennings, D., Schell, H. and Simon, G., Diffuse ferroelectric phase transitions in  $\text{Ba}(\text{Ti}_{1-y}\text{Zr}_y)\text{O}_3$  ceramics. *J. Am. Ceram. Soc.*, 1982, **65**, 539–544.
- Ciomaga, C. E., Buscaglia, M. T., Viviani, M., Buscaglia, V., Mitoseriu, L., Stancu, A. et al., Preparation and dielectric properties of  $\text{BaZr}_{0.1}\text{Ti}_{0.9}\text{O}_3$  ceramics with different grain sizes. *Phase Transit.*, 2006, **79**, 389–397.
- Mitoseriu, L., Ciomaga, C. E., Buscaglia, V., Stoleriu, L., Piazza, D., Galassi, C. et al., Hysteresis and tunability characteristics of  $\text{Ba}(\text{Zr}, \text{Ti})\text{O}_3$  ceramics described by First Order Reversal Curves diagrams. *J. Eur. Ceram. Soc.*, 2007, **27**, 3723–3726.
- Ricinchi, D. and Okuyama, M., Relationships between macroscopic polarization hysteresis and local piezoresponse of fatigued  $\text{Pb}(\text{Zr}, \text{Ti})\text{O}_3$  films within a Landau theory-based lattice model. *Appl. Phys. Lett.*, 2002, **81**, 4040–4042.
- Santos, I. A. and Eiras, J. A., Phenomenological description of the diffuse phase transition in ferroelectrics. *J. Phys.: Condens. Matter*, 2001, **13**, 11733–11740.
- Yu, Z. and Ang, C., Maxwell–Wagner polarization in ceramic composites  $\text{BaTiO}_3-(\text{Ni}_{0.3}\text{Zn}_{0.7})\text{Fe}_{2.1}\text{O}_4$ . *J. Appl. Phys.*, 2002, **91**, 794–797.
- Ye, Z. G., Relaxor ferroelectric complex perovskites: structure, properties and phase transitions. *Key Eng. Mater.*, 1998, **155–156**, 81–122.
- Kholkin, A. L., Bdikin, I. K., Kiselev, D. A., Shvartsman, V. V. and Kim, S. H., Nanoscale characterization of polycrystalline ferroelectric materials for piezoelectric applications. *J. Electroceram.*, 2007, **19**, 81–94.
- Ciomaga, C. E., Buscaglia, M. T., Mitoseriu, L., Buscaglia, V. and Nanni, P., Hysteresis and tunability characteristics of  $\text{Ba}(\text{Zr}, \text{Ti})\text{O}_3$  ceramics described by First Order Reversal Curves diagrams. *J. Opt. Adv. Mater.*, 2008, **10**, 2367–2372.